A Permanent Magnet Linear Generator for the Enhancement of the Reliability of a Wave Energy Conversion System

Marco Trapanese, *Senior Member, IEEE*, Valeria Boscaino, Giovanni Cipriani, Domenico Curto, Vincenzo Di Dio, and Vincenzo Franzitta, *Member, IEEE*

***Abstract*—In this paper, a linear generator for a highly reliable wave energy conversion system is designed and tested. In order to store energy, the system is able to produce hydrogen. The wave energy conversion system consists of an electrical linear generator, a power conversion system, and a sea-water electrolyzer. A small-scale prototype of the system is designed and built. The design is oriented to the enhancement of the system robustness and reliability and a failure mode and effects and criticality analysis are used. In order to guarantee an easy extension of the power capability of the marine plant, a modular architecture of the system is adopted. The design strategy is described. The robustness and reliability of the proposed solution are discussed. Simulation and experimental results on the prototype are shown.**

***Index Terms*—Hydrogen, sea-water electrolysis, wave energy conversion (WEC) system.**

I. Introduction

NOWADAYS, sea wave energy conversion (WEC) is increasingly attracting the attention of both the academic and industrial world. WEC systems potentially have the highest power density among all the renewable energy systems.

WEC system is made up of a mechanical converter, an electric generator, converting sea waves into electricity, and a power electronics section dedicated to the conversion, transmission, and storage of the generated electrical power. Several forecasted installations are intended to be directly connected to the grid on the coastline, thus increasing the complexity and undermining the safety of the whole system. In any case, safety and reliability are key issues to cope with for a successful marine installation and therefore the most reliable solution must be adopted. In [1], an overview of failures of existing marine plants is given. The analysis leads to identify the main causes of marine plant failures both in mechanical faults on structural parts that experience relative movements such as joints and blades, and in rotational and flip overturns as well as in faults on the power electronics subsystem when redundancy is not taken into account [1]–[15]. As a result, in the design phase, several issues must be considered to achieve robustness and reliability of the whole WEC system.

The WEC system should be resistant to harsh weather conditions keeping high reliability, high robustness, and should have a low cost, in terms of both capital and maintenance cost.

In the literature, WEC generators are usually classified as follows.

1) Oscillating water column, a partially submerged hollow structure open to the sea below the water line and equipped with air turbine.
2) Point absorbers (floating or submerged), providing a heave motion that is converted by mechanical and/or hydraulic systems in linear or rotational motion to drive electrical generators.
3) Overtopping devices (fixed or floating) that collect the water of incident waves to drive one or more low-head turbines and that are equipped with a hydraulic turbine, and surging devices that exploit the horizontal particle velocity in a wave to drive either a deflector or to generate a pumping effect of a flexible bag facing the wave front [4].

In this paper, the design of a permanent magnet linear generator (PMLG) for a highly reliable small-scale prototype of WEC for hydrogen production and storage is proposed. The proposed WEC can be classified as a point absorber and includes an electrical generator, a power electronics section, and a salt-water electrolyzer. The generation of hydrogen, which is nowadays negatively conditioned by issues related to the use of fossil fuels and fresh water consumption for its production, directly from salt-water offers the opportunity to the ocean WEC systems to become the most promising solution for hydrogen generation overcoming many issues related to hydrogen production. Furthermore, if hydrogen is stored on the marine plant, energy transmission-related issues can be efficiently avoided. In this paper, a reliability-oriented approach is adopted for the design of both the generator and the power electronics section. On the basis of the failures analysis, a robust linear generator is

Manuscript received September 11, 2017; revised December 17, 2017, February 7, 2018, and April 10, 2018; accepted May 1, 2018. Date of publication June 5, 2018; date of current version January 31, 2019. (*Corresponding author: Marco Trapanese.*)

The authors are with the Department of Energy, Information Engineering and Mathematical Model University of Palermo, 90128 Palermo, Italy (e-mail: marco.trapanese@unipa.it; valeria.boscaino@unipa.it; giovanni.cipriani@unipa.it; domenico.curto@unipa.it; vincenzo.didio@unipa.it; vincenzo.franzitta@unipa.it).

Color versions of one or more of the figures in this paper are available online at http://ieeexplore.ieee.org.

Digital Object Identifier 10.1109/TIE.2018.2838076

designed and tested. A modular architecture of the power electronics section is provided to enhance the system reliability and robustness to electronic section faults. Simulation and experimental results on a laboratory prototype are shown to validate the efficiency of the proposed design solution. In Section II, the reliability-oriented design approach is described. In Section III, simulation results are shown. In Section IV, experimental results on a small-scale laboratory prototype are shown. In Section V, conclusions are drawn.

II. Reliability-Oriented Design Approach

In order to guarantee a reliability-oriented approach, a failure mode and effects and criticality analysis (FMECA) design approach has been adopted. The analysis has been performed by considering the following steps: Decomposition of the system in subsystems, failure modes identification, failure modes causes identification, and evaluation of the effects. Several hardware solutions for each subsystem have been considered and the reliability probability of the whole system has been computed as the product of the reliability probability of each subsystem. The reliability probabilities have been deducted from literature analysis. The optimum design has been the one with maximum reliability.

A. Decomposition of the System in Subsystems

In any WEC installed offshore, there are the following structures: buoyant, mooring system, electrical generator, mechanical multiplier, power electronics, and grid connection. The buoyant is the structure directly in contact with the sea, the mooring system is the system which anchors the structure to a fixed point, the electrical generator is the electrical machine that converts the mechanical energy into electrical energy, the mechanical multiplier converts the mechanical energy of waves into a form of mechanical energy suitable as input for the electrical generator, power electronics converts the electrical energy produced by the electrical generator into a form of electrical energy that can be delivered to the grid, and finally grid connection is the connection between the generator and the grid. Consequently, for the FMECA analysis, the system has been decomposed in the above-described subsystems (buoyant, mooring, electrical generator, mechanical multiplier, power electronics, and grid connection).

For each subsystem, several solutions have been considered and for each solution the failure modes, the failure occurrence probability, the effects and the criticality analysis have been evaluated. Below, we refer to these quantities as FMECA parameters. In Table I, various subsystems with various examined solutions are shown.

TABLE I
FMECA Parameters

Subsystem	Solutions	Failure time	Failure mode
Buoyant	Symmetrical	6 M	Flip mode
	Asymetrical	5 Y	Sink
mooring	Rigid	5Y	Loss of buoyant
	Elastic	10Y	Loss of Buoyant
electrical generator	Rotating with mechanical multiplier	1Y 5Y	Mechanical failure Loss of phases
	PMLG direct coupling with no cogging force induced vibrations	5Y	Mechanical vibration, Loss of phases and magnetization loss
mechanical multiplier	Presence	1Y	Mechanical failure
	Absence	Infinite	None
power electronics	Centralized	5Y	Loss of function
	Modular	5Y for each module	Partial loss of function
Grid connection	Presence	5Y	Loss of function
	Absence (use of energy storage)	Infinite	None

B. Subsystems FMECA Parameters Estimation

Mathematically, reliability is defined as follows:

$$P_{\text{rel}} = 1 - P_{\text{fail}} \tag{1a}$$

where P_{rel} is the reliability index and P_{fail} is the probability to fail. Therefore, reliability index is a probability. The failure probability is the probability that a specific item, such as a piece of equipment, material, or system fails at a certain time interval in absence of maintenance activities. Generally speaking, the reliability of a device can be computed by estimating P_{fail} through a statistical analysis that gives the statistical frequency of faults. It is well established that the occurrence of fails in a device follows the so-called "bath-tube" curve. It has been generally shown that P_{fail} is higher in the beginning and in the end of the lifetime of product, while in the central period there is a low plateau. However, in absence of a statistical analysis, this P_{fail} cannot be obtained accurately. In this paper, we assumed that P_{fail} can be computed by analogy considering the declared maintenance time cycles for any subsystem composing a complex system as follows:

$$P_{\text{fail}} = t/T_m \tag{1b}$$

where t is time and T_m is the declared maintenance time for each subsystems. Equation (1b) means that the probability of a failure increases with time and that beyond the maintenance time it is certain that each subsystem will fail. Equation (1b) overestimates P_{fail} during the lifetime of the device but correctly estimates the expected lifetime. As a result, in order to give an estimation of P_{fail}, the maintenance cycle of each subsystem is needed.

With reference to the solution of the buoyant, we have considered two solutions: One with an asymmetrical buoyant (with a top and low part of the buoyant) and another with a full rotational symmetry (a cylinder, an ellipsoid, a sphere, etc.), we assumed that the failure modes for the buoyant are the sinking mode and the flip and overturns mode, we estimated the probability of the sinking mode by using the typical survivability period of a boat and the probability of the flip and overturns by using the typical time of this event for the experimental WEC reported in the literature. The effect of this event is the complete loss of

function in the case of asymmetrical buoyant. The criticality of this event is maximum.

With reference to the mooring system, we have considered two solutions: A rigid mooring and an elastic one, we assumed that the failure modes for mooring is essentially the loss of the buoyant and we estimated the probability of the loss of the buoyant by examining the typical survivability time of measurements buoyant deployed around Italy. The effect of this event is the complete loss of function. The criticality of this event is maximum.

With reference to the electrical generator, we have considered two solutions: One based on a rotating generator and the other one on PMLG, we assumed that the failure modes of the generator are the loss of function due to mechanical failures induced by vibrations, the loss of some phases, and the loss of the magnetization. Because of the fact that the generator is not directly connected to the grid, we neglected the effect of overvoltages, short circuits, and thermal overloads. We estimated the failure by examining the typical data of electrical machines reported in the literature. The effect of mechanical failure as well as of the magnetization is usually a complete loss of function, on the contrary, the loss of some phases is a reduction of phases. The subsystem is critical for energy production.

With reference to mechanical multiplier, we have analyzed two different options: In the case of a rotating generator, a mechanical multiplier and coupling is needed, on the contrary in the case of PMLG the use of the mechanical multiplier can be avoided. We have assumed that the failure mode of the multiplier is the loss of function and estimated the failure probability of the multiplier by assuming the maintenance time cycle used in wind turbines (one year). The effect of mechanical failure in the multiplier is usually a complete loss of function. The subsystem, if used, is critical for energy production.

With reference to power electronics, we have analyzed two different options: A centralized option with one single power converter and a decentralized option with several converting units. We estimated the failure probability of the power electronics by using the lifetime data available for commercial converters. The effect of a failure in a centralized approach is usually a complete loss of function, on the contrary, if a modular approach is used, there is a reduction of function. The subsystem, if used in the centralized version, is critical for energy production, on the contrary, in the use of a modular solution, in case of failure of a single module, we have a reduction of function.

With reference to grid connection, we considered two options: The presence of a marine connection with the use of an ac cable and the absence of a connection with the use of hydrogen-based storage. The effect of a failure in the grid connection, if used, is a complete loss of function.

In Table I, the FMECA parameters are reported. The table has been based on publically available data considering the best performance for each type of failure [1], [3], [4], [8], [10], [13].

C. Reliability Optimization

Table I clearly shows that the most critical aspects in designing a WEC are the mechanical behavior and the flip and rotational overturns (these failure modes present the shorter failure time). The mechanical problems are caused by internal and external mechanical vibrations. Internal vibrations are caused by cogging force and external vibrations by sea-waves. Electronic is also prone to some failures but the problem can be solved with some degree of modularity and redundancy. As a result, we decided to focus our attention on the mechanical properties of the PMLG and to design our systems by searching the following condition:

$$D \text{ for which Min } (\mathrm{P_{fail}}) \tag{2}$$

where D is the set of parameters that minimizes the probability of failing. The analysis of Table I clearly shows that the best solution is based on a PMLG with low vibration, with symmetrical properties in the buoyant, without mechanical multiplier and grid connection. The absence of grid connection implies the adoption of an energy storage method. As a result, the generator must be designed to mechanically sustain the maximum possible wave and to minimize the cogging force.

The optimization procedure has been split in several subprocedures.

The design of the generator consisted in the following four steps:

1) preliminary sizing of the generator;
2) parametric analysis of the structures determined in step 1 by using a three-dimensional FEM simulator;
3) estimation of the induced mechanical vibration by considering the parasitic effects due to cogging force;
4) optimization.

The preliminary sizing of the generator gives the general dimensions of the device. The parametric analysis specifies the structure of the generator within the frame of the general dimensions obtained in step 1. It was obtained a double-sided planar structure with skewed magnets placed on the mover [see Fig. 1(a) and (b)]. In the designed prototype, the slot pitch is fixed at 25.5 mm so that two consecutive inductor north poles overlap six stator slots. Thanks to the fact that a double layer winding is installed and that the pole pitch can be easily varied, the experimental prototype allows several connections of the stator winding coils, as a result, several configurations can be and have been preliminarily tested to evaluate the effects on the cogging force. A distributed winding was the one that minimized in transient regime the cogging torque and was therefore adopted. In Fig. 2, the level of the cogging force for the two types of winding is shown. The better performance of the distributed winding is due to the better distribution of the magnetic field in the ferromagnetic circuit.

The skewing angle was the parameter to be determined in the optimization procedure in order to minimize the cogging force and the induced vibrations. The voltage was produced by the wave induced motion of the mover with respect to the armature.

The estimation of the induced mechanical vibration was performed by evaluating the cogging force generated by several assemblies of magnets on the mover of the linear generator.

Finally, the optimization step has given the best geometry that can be used in order to have the maximum reliability and therefore the minimum cogging force and the maximum voltage

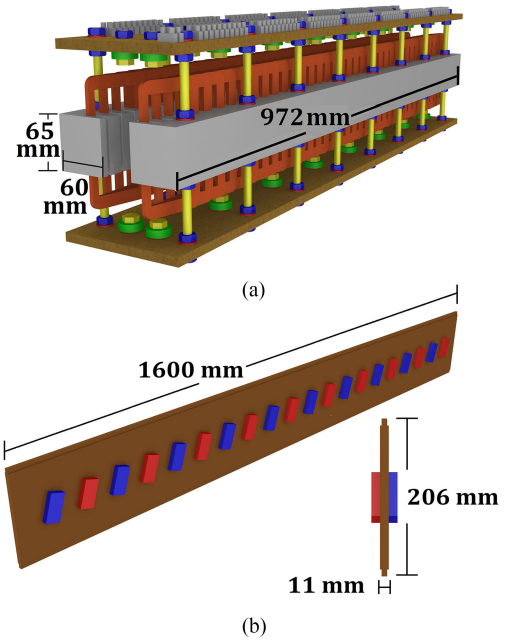

Fig. 1. (a) Armature of the generator [16]. (b) Mover with the skewed magnets [16].

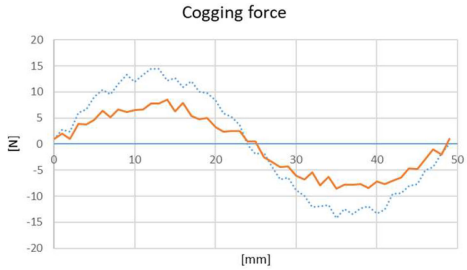

Fig. 2. Cogging force. On the *y*-axis is recorded the cogging force and on the *x*-axis the displacement. The dotted line shows the cogging force in the case of concentrated winding (best case), the continuous one refers to the distributed winding (best case).

and efficiency. The optimization was performed by a Monte Carlo sampling of several structures [see Fig. 3(a) and (b)].

A skew angle of 70°, the value in which the maximum overlap between the surface of magnets and teeth is achieved, was chosen. In [16], it has been also shown how such a large angle reduces the output voltage only slightly.

As a result, in order to enhance the reliability and safety of the whole WEC system, a generator, that is robust against rotational and flip overturns, presents no moving parts directly exposed to the sea and has some kind of redundancy and modularity in the electronic section, must be chosen.

Consequently, the proposed WEC system presents the following.

1) An intrinsic axis-symmetry to avoid overturn and the whole WEC system is based on a linear generator minimizing the relative motion between the external parts and thus minimizing structural faults.
2) An internal mounted PMLG that mitigates the external vibration induced by sea-waves (see Fig. 4) and has a skewed magnet disposition that minimizes internal vibration (cogging force) (see Fig. 2).
3) A voltage level that allows to produce hydrogen from salt water with a high level of redundancy. The voltage is generated by the wave-induced motion of the mover.

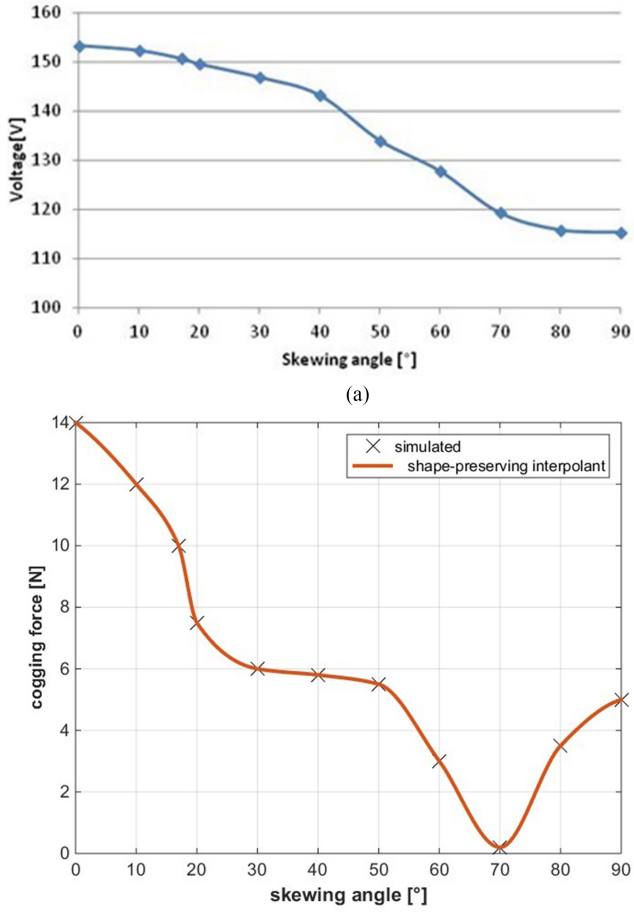

Fig. 3. (a) (Upper diagram) Output voltage versus skewing angle. (b) (Lower diagram) Cogging force versus skewing angle [16].

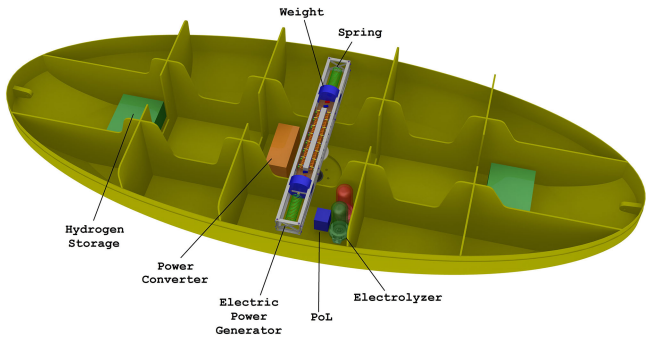

Fig. 4. WEC system structure. A cross-sectional view. The system is completed by an upper shell having the same shape of the lower shell and keeping a cylindrical symmetry.

The proposed WEC system is conceived to produce hydrogen from salt-water and store the produced hydrogen on-board thus avoiding power routing from the marine plant which is the main

TABLE II
FUNDAMENTALS OF THE PROPOSED RELIABILITY-ORIENTED APPROACH

PROBLEMS	ADOPTED SOLUTIONS
Rough weather	**Buoyant systems** ▪ Intrinsic symmetry to achieve immunity against overturn, flip and rotation events **Electric generator** ▪ Minimization of the relative motion between the external parts
Electronic or control section faults	**Power Electronics System** ▪ High reliability of the power electronics converters
Low capital and maintenance cost	**Power Electronics System** ▪ Modularity ▪ Low components' count ▪ Redundancy ▪ Efficient size of power modules ▪ High reliability ▪ Commercial components
Safety and transport related issues	**On-board hydrogen production and storage** **Electric generator** ▪ Minimization of the relative motion between the exposed parts to prevent from damages to the neighborhoods

TABLE III
LINEAR GENERATOR PARAMETERS

Machine section	Parameters
Stator	▪ Size: 60x972x65 mm ▪ 126 iron sheets ▪ Sheet's thickness 0.5 mm ▪ 39 slots ▪ Internal slot width: 12 mm ▪ 8 holes (diameter 10,5 mm) for the tightening of the sheets with bolts
Mover	▪ Alternating magnets interspersed with soft iron poke pieces mounted on a Bakelite sheet. ▪ Sheet size: 1600x11x206 mm
Windings	▪ Enameled copper wire 0.5 mm diameter ▪ 375 turns ▪ Rectangular shape ▪ 85x135 mm ▪ Coil weight: 278 g
Permanent magnets	▪ Ne-Fe-B ▪ 40 magnets ▪ Size: 60x30x15 mm ▪ Weight: 205.2 g

hindrance to the robustness of existing marine plants. In Table II, design criteria are listed. Fig. 4 shows the WEC system structure obtained by the optimization analysis.

D. Linear Generator

In [17], an overview of Italian coast power capability is given and a location with a 3.9 kW/m wave power per meter has been chosen as potential site of installation. In order to reproduce this condition, the laboratory prototype has been equipped with a mover, whose length is equal to 160 cm and a stator of 97.1 cm length. Therefore, a 62.9 cm is considered to size the power rating of the generator. Considering the mechanical efficiency, the power rating of the generator is equal to 1.22 kW. The PMLG obtained by the optimization procedure is a bilateral generator equipped with two stators and has been shown in Fig. 2.

Although, for this application, eddy currents frequency is very low, the two stators have been laminated. In order to minimize the eddy currents, each stator core (60 × 972 × 65 mm) has been assembled overlapping 126 AISI 1008 steel sheets of 0.5 mm thickness. In this way, a lamination direction orthogonal to the mover direction has been obtained, also allowing an easy assembling process.

Each internal slot has a 12 mm width to house two windings. External three slots have an 8 mm width. About 13.5 mm teeth are built, except the first and last tooth that measure 7 mm. The stator is assembled by two tables of Bakelite, thus achieving an overall size of 970 × 160 × 11 mm.

The mover was assembled by alternating 40 Neodymium–Iron–Boron (Nd–Fe–B) permanent magnets, interspersed with soft iron pole pieces mounted on a Bakelite sheet. The magnets are stacked in pairs. Consequently, opposing magnetomotive forces drive the flux through the soft iron. Each magnet is protected by nickel coating. The Bakelite sheet size is 1600 × 11 × 206 mm and includes 40 hallows for magnets housing.

Copper coils, featuring 375 turns of rectangular shape with an average size of 85 × 135 mm, are manufactured by enameled copper wire of 0.5 mm diameter. Each coil weighs 278 g. In each side of the armature, 36 coils are arranged for a total number of 72 coils. A three-phase star connection is implemented. The linear generator is arranged in a six-phases stator windings configuration. The parameters of linear generator are summarized in Table III and a thorough numerical and experimental analysis of the proposed generator is reported in [16]. As far as the reliability is concerned, the leading feature is the cogging force.

E. Electrolyzer

A laboratory prototype of salt-water electrolyzer has been designed and tested. The production of hydrogen has been validated by a low-power fuel cell stack. The supply voltage and the load current requirements have been measured to size the power electronics section and the modular architecture. The operating voltages span 10–30 V range and current is in the range 0.27–0.96 A.

In [18], a detailed overview of sea water electrolysis and a comparison of alkaline, brine, and sea-water electrolysis processes are given.

F. Power Electronics Section

The power electronics section is dedicated to the production of hydrogen. Therefore, it must essentially provide a constant dc voltage under the presence of a very distorted waveform produced by the linear generator. The setup of the circuit is shown in Fig. 5. High level of modularity is provided to enhance the system redundancy and reliability. A diode rectifier bridge is modeled and designed. A modular architecture is conceived to both increase the reliability of the system and to further extend the overall power for the forecast marine installation. Each

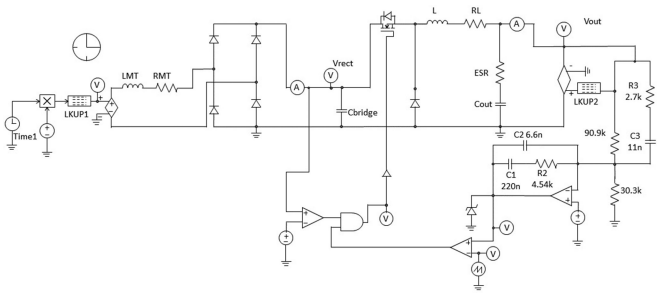

Fig. 5. Simulation setup of the power electronics section.

power module consists of a point of load dc–dc converter and a sea-water electrolyzer. Modularity is limited to the point of load converters to limit the capital and maintenance cost of the whole marine plant. Furthermore, in order to limit the complexity of the whole system, a diode rectifier bridge is implemented instead of more advanced rectifier topologies, self- or control-driven based on Metal-Oxide-Semiconductor Field-Effect Transistor (MOSFETs) or Insulated Gate Bipolar Transistor (IGBTs). The module should supply the sea water electrolyzer during the wave burst thus providing a short-term energy storage between consecutive waves.

A diode bridge is included in the power system interface model as the front-end power converter.

Although the use of diodes, in this case, determines an increase of the power losses of the system, it allows a significant simplification and a cost reduction.

A capacitive energy storage element is included at the output of the rectifier section. Yet, the capacitor value should be limited to avoid instability and oscillations due to the inductive behavior of the linear generator. The minimum voltage value of the power electronics section is determined by the nominal voltage of the electrolyzer prototype (20 V). According to experimental results on the linear generator, the maximum open-circuit voltage value is equal to 130 V. The maximum voltage of 130 V depends on simulation and experimental results on the linear generator. In particular, it depends on the mover acceleration. Tests are carried out on the laboratory prototype with several weights, as reported in the simulation and experimental results section. The laboratory prototype is not equipped with anchor springs and ballasts. For marine installation, the buoyant system will include anchor springs and ballasts, which will be designed to obtain the same maximum voltage value of 130 V according to the foreseen wave length, amplitude, and sea-state.

The capacitor theoretically charges up to the burst peak of 130 V. The storage element will supply the electrolyzer through the buck converter interposed between them. If the input voltage of the buck converter drops below 25 V, the converter is disabled and the output storage element supplies the electrolyzer discharging toward zero value.

In order to design the C_{rect} capacitor, the following design relationship is considered:

$$P_{\text{out}} T_{\max} = \Delta Ec = \frac{C_{\text{rect}}}{2} \left[V^2\right]_{25}^{130} \tag{3}$$

where P_{out} is the electrolyzer nominal power and $T_{\max}$ is the maximum self-supply period.

On the basis of (3), the capacitor value is fixed at 3.3 mF to achieve a 2.2 s self-supply interval. After 2.2 s, the buck converter will be disconnected. The output capacitor C_{out} will discharge at a constant current rate, which is the electrolyzer current.

Among dc–dc converters, nonisolated topologies are focused on to limit the cost of each power module. Among nonisolated topologies, input-inductive converters are discarded. A buck converter is designed. The buck converter is designed to ensure an adequate power supply of the electrolyzer, avoiding instabilities and oscillations, during the wave burst [19]. Each module includes a buck converter and the sea wave electrolyzer. The nominal supply voltage of the electrolyzer is set at 20 V. A continuous conduction mode of operation is designed not overloading the rectifier capacitor during the burst wave. The minimum converter current is fixed at 0.2 A, according to experimental results on the laboratory prototype of the electrolyzer. A voltage mode pulsewidth modulation control network is designed. The switching frequency is fixed at 100 kHz. The inductance value is designed by forcing a CCM operation, as given by the following:

$$L > \frac{V_{\text{out}}(1 - D_{\min})}{2 f_{\text{sw}} I_{\text{omin}}} \tag{4}$$

where V_{out} is the nominal output voltage, I_{omin} the minimum output current fixed at 0.2 A, $D_{\min}$ the minimum duty-cycle value over the whole operating range and, consequently, at the maximum operating voltage of 130 V, corresponding to the measured peak value of the open-circuit voltage generated by the linear PMG. Equation (4) implies that a 0.42 mH critical inductance is obtained and a 1 mH inductance value is selected to ensure CCM over the whole operating range. The open-loop damping factor is given by the following:

$$\xi = \frac{R_{\text{tot}}}{2} \sqrt{\frac{C_{\text{out}}}{L}}. \tag{5}$$

In order to avoid stability and compensation issues deriving from an extremely low resonant frequency, the C_{out} is fixed at 1 mF thus achieving a 0.4 open-loop damping factor.

The control system is based on a type III error amplifier network. Resistive parasitic elements are included. As shown by Fig. 6, a phase margin of 61.5°, a gain margin of 28.9 dB, and a 1 kHz bandwidth are achieved under the maximum operating voltage and minimum output current. Performances are adequate to the specific application and a robust control against parameters and components tolerances is achieved.

III. Simulation Results

Simulation results are here presented to validate the proposed design approach and to show that the system has the capability to produce a voltage level to supply the electrolyzer. It is demanded to the experimental sets reported in Section IV the validation of the design approach. The measured open-circuit voltage generated by the linear PMG is imported as a look-up table in the simulation setup in order to test the power sec-

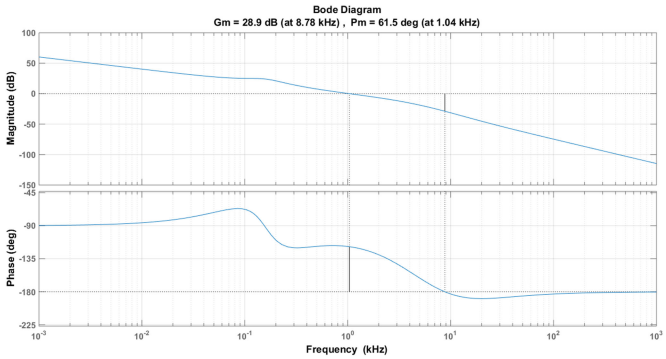

Fig. 6. Bode diagrams (magnitude and phase) of the open-loop transfer function of the buck converter at $V_{\rm in} = 130$ V and $I_{\rm load} = 0.2$ A including the type III error amplifier.

tion as closely as possible to its actual working conditions. The generator phase is modeled by a series connection of an inductance *LMT* and a resistor *RMT*. According to experimental results LMT = 154 mH, RMT = 36.6 Ω.

The electrolyzer is modeled by a look-up table. The electrolyzer is supplied by the output voltage of the power section and a constant current is drawn according to the electrolyzer data. It is assumed that below 10 V, the electrolyzer is disconnected from the power section.

The rectifier bridge and the buck power converters are modeled including loss parameters.

When the output voltage of the rectifier bridge falls below 25 V, the buck converter is disconnected to avoid oscillations and the electrolyzer is supplied by the output capacitor of the buck converter itself.

Two cases are simulated. First, simulation results under a constant acceleration of the mover are presented, then an oscillating buoyant system is assumed and simulation results under a 20° maximum oscillation are presented. As it will be shown by simulation results, a continuous supply of the electrolyzer is ensured under both test conditions during the sea-wave burst.

A. Simulation Results Under Uniform Acceleration

The simulation was performed by assuming that a constant acceleration of 1.2 m/s^2 is obtained by applying a constant mechanical load to the mover. The measured open-circuit voltage across a single phase of the linear generator is shown in Fig. 7. A maximum value of 130 V is obtained, which is adequate to supply the load power equipment. According to the six-phases machine structure, three couple of phases are in phase opposition. Therefore, even a three-phase configuration could be implemented by properly connecting the six-phases of the linear generator.

The measured open-circuit voltage is imported in the simulation setup to test the power electronics section. Simulation results are shown in Fig. 8. From the top to the bottom screen, the open-circuit voltage V_{01}, input rectifier voltage $V_{\rm inrect}$, the output rectifier voltage $V_{\rm rect}$; the output voltage $V_{\rm out}$, and the electrolyzer current $I_{\rm load}$ are shown. The nominal voltage of 20 V is controlled over the whole sea-wave burst. The electrolyzer is properly supplied at its nominal conditions during the whole sea-wave burst. When the burst extinguishes, the power module is disconnected from the rectifier and the output capacitor discharges over the electrolyzer, which draws a variable current from the power system according to the actual capacitor voltage, as to experimental measures.

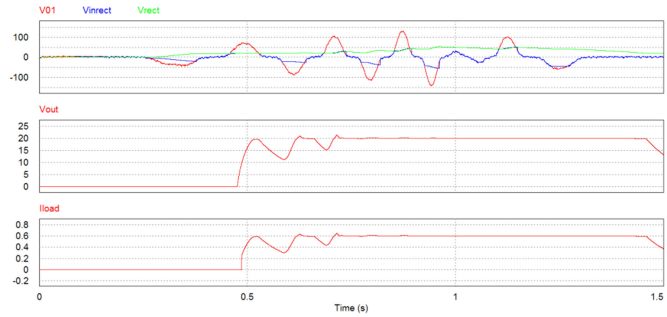

Fig. 7. Measured open-circuit voltage across a single phase of the PMLG under a 1.8 kg weight.

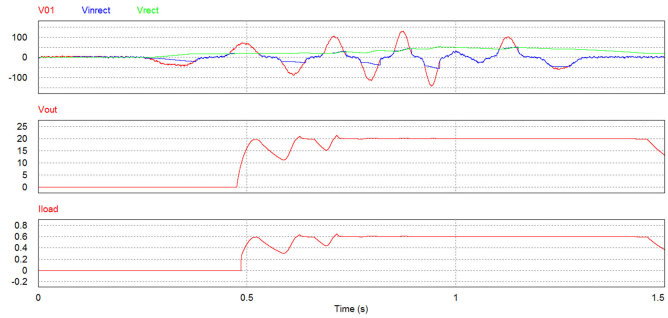

Fig. 8. Simulation results under an emulated sea-wave burst. From the top to the bottom screen, the open-circuit voltage V_{01}, input rectifier voltage $V_{\rm inrect}$ the output rectifier voltage $V_{\rm rect}$; the output voltage $V_{\rm out}$, and the electrolyzer current $I_{\rm load}$ are shown.

B. Simulation Results Under an Oscillating Buoyant System

In this case, a buoyant system is assumed. The buoyant system is assumed to have the mover translating along the short dimension (see Fig. 4). The mover is equipped with an 80 kg mechanical load and a spring to trace back the mover to its reference position after the sea-wave burst. In this case, an oscillation of the buoyant system is accounted for and a variable acceleration of the mover is obtained.

It is assumed a sinusoidal buoy angle with respect to the horizontal line

$$\vartheta(t) = \vartheta_M \sin[\omega t]. \tag{6}$$

The resultant force applied to the mover along the inclined plane determined by $\vartheta(t)$ is given by the following:

$$F_{p||} - F_{\rm frict} + F_{\rm cogg} - F_{\rm el} - F_{\rm spring} = M\frac{d^2 r}{dt^2} \tag{7}$$

where *M* includes the mechanical load and the mover mass, *r(t)* is the instantaneous mover position alongside the inclined plane,

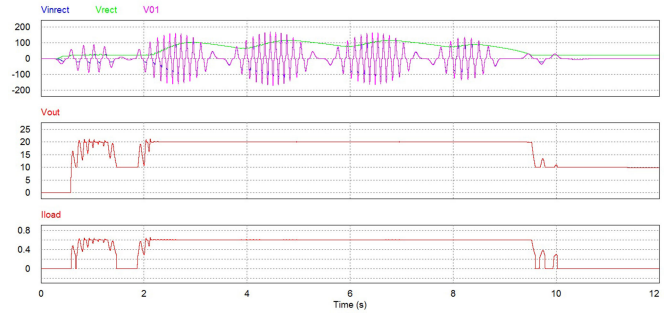

Fig. 9. Simulation results under oscillations of the buoyant system. From the top to the bottom screen, the open-circuit voltage V_{01}, input rectifier voltage V_{inrect} the output rectifier voltage V_{rect}; the output voltage V_{out}, and the electrolyzer current I_{load} are shown.

$F_{p||}$ is the parallel component of the weight, F_{frict} is the friction force, F_{cogg} is the cogging force, F_{spring} is the spring force, and F_{el} is the electrical force. The parallel component of the weight is given by the following:

$$F_{p||} = -Mg\,\sin\vartheta\,(t)\,. \tag{8}$$

The friction force is given by the following:

$$F_{\mathrm{frict}} = -\mathrm{segn}\left[v\,(t)\right]\mu Mg\,\cos\vartheta\,(t) \tag{9}$$

where μ is the friction coefficient.

The cogging force originates from the interaction between the last magnet and the last tooth and from the interaction between the magnet and the tooth or slot and can be computed by through a look-up table.

The braking electrical force due to the electromechanical conversion is given by the following:

$$F_{\mathrm{ele}} = \frac{1}{v\,(t)}\left\{R_T\sum_{j=1}^{6} i_j^2\,(t) + L\sum_{j=1}^{6} i_j\,(t)\,\frac{di_j\,(t)}{dt}\right\} \tag{10}$$

where R_T is the total resistance, L the windings inductance, i_{j} the current through the *j*th windings.

The spring force is given by the following:

$$F_{\mathrm{spring}} = -K\left[r\,(t) - r_{\mathrm{rif}}\right] \tag{11}$$

where *K* is the spring constant and r_{rif} is the reference position of the mover.

The differential equations are solved by the backward Euler method in order to obtain the laws of motion and the open-circuit voltage.

The open-circuit voltage has been simulated assuming two oscillations of the buoyant system and a maximum buoy angle of 20°.

Simulation results are shown in Fig. 9. From the top to the bottom screen, the open-circuit voltage V_{01}, input rectifier voltage V_{inrect}, the output rectifier voltage V_{rect}, the output voltage V_{out}, and the electrolyzer current I_{load} are shown.

The electrolyzer is properly supplied during intermediate sea-wave bursts. The first burst features too low amplitude and the rectifier voltage drops below 25 V. Consequently, the electrolyzer is supplied by the buck converter output capacitor.

Fig. 10. Test bench of the wave energy conversion system

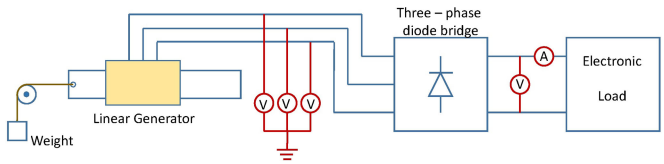

Fig. 11. Scheme of the used test bench.

IV. Experimental Results

The experimental tests aimed at both validating the proposed design in terms of consistency between the designed voltage output and current output and the experimental ones and estimating the number of electrolyzing module that the system can supply. Figs. 10 and 11 show respectively the experimental setup and a scheme of the used test bench. The experiments consisted of letting the mover moving driven by various falling weights and recording the output voltage generated by the generator. The laboratory prototype is housed at the University of Palermo. The prototype of the linear generator, in a three-phase connection is connected to the power electronics system. The power electronics system under test is a three-phase diode bridge loaded by a current generator. The number of modules and hydrogen production rate is sized by analyzing the experimental results. A LeCroy WavePro 7200A Digital Scope for data postprocessing measures phase voltage signals and the output voltage of the rectifier stage. A weight is applied to the linear generator in each experiment.

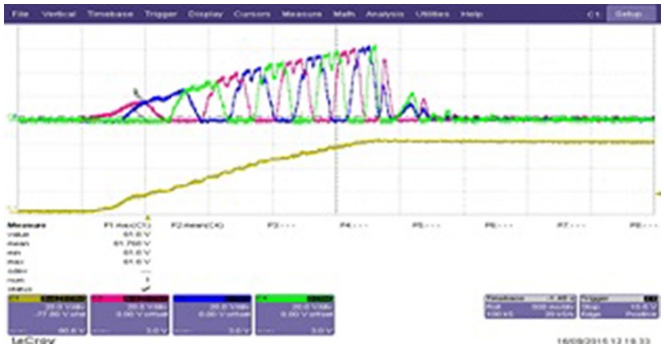

Fig. 12. Experimental results under a 1.8 kg mechanical load and open-circuit configuration at the rectifier output. Phase voltages at the rectifier input sections (Ch2, Ch3, Ch4, 20 V/div) and the output rectifier voltage (Ch1, 20 V/div) are shown. Time base is set at 500 ms/div.

The tests reported consisted of the following:

1) recording of open-circuit voltage with a 1.8 kg falling weight;
2) recording voltage with a 5.0 kg falling weight and an ohmic load of 1 A;
3) recording voltage with a 10.0 kg falling weight and an ohmic load of 3.5 A.

A. Open-Circuit Voltage With a 1.8 kg Falling Weight

In Fig. 12, experimental results under a 1.8 kg mechanical load weight and open circuit at the rectifier output section are presented. On Ch2, Ch3, and Ch4 (20 V/div) the half-sinusoid three-phase signals are measured at each phase terminal of the linear generator. The open-circuit voltage at the rectifier output section is measured on Ch1 (20 V/div). The common reference is the ground reference at the rectifier output and therefore half-sinusoidal signals are measured at the input section. The measured peak value of the output voltage is equal to 61.8 V. The designed value for this condition was 70.2 V.

The rectifier output voltage is constant after the wave pulse because of the open-circuit configuration.

B. Voltage With a 5.0 kg Falling Weight and an Ohmic Load of 1 A

In Fig. 13, experimental results under a 5 kg mechanical load weight and 1 A constant load current at the rectifier output section are presented. On Ch2, Ch3, and Ch4 (20 V/div) the half-sinusoid three-phase signals are measured at each phase terminal of the linear generator. The open-circuit voltage at the rectifier output section is measured on Ch1 (20 V/div). The measured peak value of the output voltage is equal to 76 V.

The designed value for this condition was 82.3 V.

The rectifier output is loaded by a constant current, contributing to the output capacitor discharge during the decaying interval of the wave burst.

The wave burst energy delivered to the electronics load is given by the following:

$$E_{\text{burst}} = \frac{V_{\text{peak}} I_{\text{load}}}{2} T_{\text{burst}}. \tag{12}$$

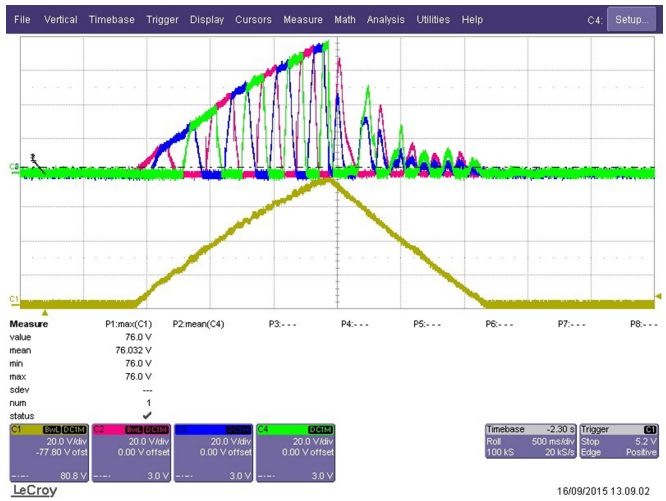

Fig. 13. Experimental results under a 5 kg mechanical load and 1 A constant load current at the rectifier output. Phase voltages at the rectifier input sections (Ch2, Ch3, Ch4, 20 V/div) and the output rectifier voltage (Ch1, 20 V/div) are shown. Time base is set at 500 ms/div.

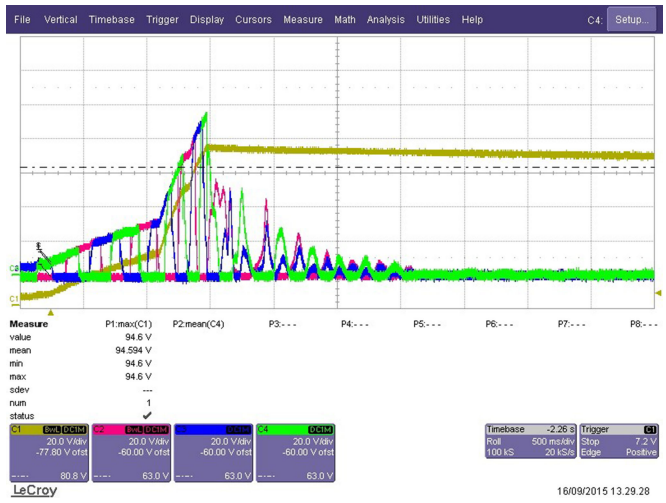

Fig. 14. Experimental results under a 10 kg mechanical load and 3.5 A load current at the rectifier output. Phase voltages at the rectifier input sections (Ch2, Ch3, Ch4, 20 V/div) and the output rectifier voltage (Ch1, 20 V/div) are shown. Time base is set at 500 ms/div.

From experimental results, under a 5 kg mechanical load, the peak output voltage value is equal to 76 V. The load current is fixed at 1 A. The burst duration is equal to 2.8 s.

If a 4 s interval between waves is assumed, according to studies in the Mediterranean sea, one module can be properly supplied by the small-scale prototype of WEC.

C. Voltage With a 10.0 kg Falling Weight and an Ohmic Load of 3.5 A

In Fig. 14, experimental results under 10 kg mechanical load and 3.5 A load current at the rectifier output section are presented. As derived by experimental results, the wave burst energy delivered to the load equals 480 J. From (7), the suitable number of modules is derived. In this case, a number of five

modules could be efficiently supplied in a continuous supply strategy. If a pulsed supply strategy is assumed, up to 13 modules can be efficiently supplied. The recorded voltage was 95 V, the designed one 101.2 V. The difference between the designed value and the experimental one is likely due to an underestimation of mechanical friction. However, it is largely within the usual error obtained in numerical analysis.

D. Evaluation of the Tests and System Performances

The tests, whose results are depicted in Figs. 12–14, show that the experimentally measured voltage values and the designed ones agree within 10%. It confirms that the chosen design approach can satisfactorily describe the proposed linear generator to be used in the WEC system.

As shown by experimental results, the small-scale prototype is suitable for hydrogen production and storage from sea water. According to the design procedure, in the case of a Mediterranean environment, one power module is adequately supplied if a continuous working strategy is adopted. If hydrogen production is devoted to storage, a number of three modules can be efficiently supplied during wave burst under the worst case. Modularity increases the system redundancy and therefore the reliability of the whole system in case of a module fault. The modularity of the system allows the designer to easily upgrade the power level and hydrogen production rate of the whole marine plant.

V. Conclusions

In this paper, a prototype of a PMLG for a wave energy converter for hydrogen production and storage was designed and tested. Based on a preliminary analysis of failures and faults of existing marine plants, the proposed design strategy was oriented to enhance the system reliability and robustness and to lower the capital and maintenance cost.

The WEC system for on-board hydrogen production and storage was designed. Consequently, no connection to the grid is required. The proposed mechanical structure is immune to rotation and flip events. By the proposed buoyant geometrical structure and intrinsic symmetry, the designed WEC is well suited to face with storms and rough weather conditions. The linear PMG is connected to a rectifier bridge and a modular architecture of the point of load converters was proposed and efficiently sized on the basis of experimental results for the forecast marine installation. A point of load dc–dc converter and a sea-water electrolyzer were included in each power module. The proposed power module architecture and size was oriented to enhance the reliability of the power conversion section, limiting the cost and components number of the power plant and ensuring an adequate supply strategy for hydrogen storage. As shown by experimental results, under the worst-sea-wave conditions, a number of three modules were properly supplied.

References

[1] V. Boscaino, G. Cipriani, V. Di Dio, V. Franzitta, and M. Trapanense, "Experimental test and simulations on a linear generator-based prototype of a wave energy conversion system designed with a reliability-oriented approach," *Sustainability*, vol. 9, no. 1, 2017.

[2] A. F. de O. Falcão, "Wave energy utilization: A review of the technologies," *Renewable Sustain. Energy Rev.*, vol. 14, no. 3, pp. 899–918, 2010.

[3] A. Clément *et al.*, "Wave energy in Europe: Current status and perspectives," *Renewable Sustain. Energy Rev.*, vol. 6, no. 5, pp. 405–431, 2002.

[4] J. Brooke, *Wave Energy Conversion*, vol. 6. Amsterdam, The Netherlands: Elsevier, 2003.

[5] F. O. Rourke, F. Boyle, and A. Reynolds, "Tidal energy update 2009," *Appl. Energy*, vol. 87, no. 2, pp. 398–409, 2010.

[6] M. C. Carcas, "The OPD Pelamis WEC: Current status and onward programme (2002)," *Int. J. Ambient Energy*, vol. 24, no. 1, pp. 21–28, 2003.

[7] R. Yemm, D. Pizer, C. Retzler, and R. Henderson, "Pelamis: Experience from concept to connection," *Philosoph. Trans. Roy. Soc. A*, vol. 370, no. 1959, pp. 365–380, 2012.

[8] T. Watabe and H. Kondo, "Hydraulic technology and utilization of ocean wave power," *Proc. JFPS Int. Symp. Fluid Power*, vol. 1989, no. 1, pp. 533–540, 1989.

[9] P. Devine-Wright, "Enhancing local distinctiveness fosters public acceptance of tidal energy: A {UK} case study," *Energy Policy*, vol. 39, no. 1, pp. 83–93, 2011.

[10] A. Falcão, "Developments in oscillating water column wave energy converters and air turbines," in *Renewable Energies Offshore*. Boca Raton, FL, USA: CRC Press 2015, p. 3.

[11] R. Henderson, "Design, simulation, and testing of a novel hydraulic power take-off system for the Pelamis wave energy converter," *Renewable Energy*, vol. 31, no. 2, pp. 271–283, 2006.

[12] G. J. Dalton, R. Alcorn, and T. Lewis, "Case study feasibility analysis of the Pelamis wave energy convertor in Ireland, Portugal and North America," *Renewable Energy*, vol. 35, no. 2, pp. 443–455, 2010.

[13] T. Crescenzi, D. Nicolini, A. Fontanella, and L. Sipione, "Caratteristiche costruttive dei sistemi OWC e dei power take-off a questi applicabili (Structural features of OWC systems and of power take off connectable to the latter)," Italian Nat. Agency for New Technol., Energy and Sustain. Econ. Develop. (ENEA), Rome, Italy, 2013.

[14] L. Margheritini, D. Vicinanza, and P. Frigaard, "SSG wave energy converter: Design, reliability and hydraulic performance of an innovative overtopping device," *Renewable Energy*, vol. 34, no. 5, pp. 1371–1380, 2007.

[15] A. Weinstein, G. Fredrikson, M. J. Parks, and K. Nielsen, "AquaBuOY—The offshore wave energy converter numerical modeling and optimization," in *Proc. Oceans.*, 2004, vol. 4, pp. 1854–1859.

[16] M. Trapanese, G. Cipriani, D. Curto, V. Di Dio, and V. Franzitta, "Optimization of cogging force in a linear permanent magnet generator for the conversion of sea waves energy," in *Proc. IEEE Int. Elect. Mach. Drives Conf.*, 2015, pp. 769–773.

[17] L. Liberti, A. Carillo, and G. Sannino, "Wave energy resource assessment in the Mediterranean, the Italian perspective," *Renewable Energy*, vol. 50, pp. 938–949, 2013.

[18] H. Abdel-Aal, K. Zohdy, and M. A. Kareem, "Hydrogen production using sea water electrolysis," *Open Fuel Cells J.*, vol. 3, pp. 1–7, 2010.

[19] V. Boscaino *et al.*, "A small scale prototype of a wave energy conversion system for hydrogen production," in *Proc. 41st Annu. Conf. IEEE Ind. Electron. Soc.*, 2015, pp. 3591–3596.

Marco Trapanese (SM'15) received the Graduate degree in Physics, in 1988 and electrical engineering, in 2003, the Ph.D. degree in electrical engineering, in 1997 and is specialized in medical physics, in 2015.

He is an Associate Professor of Electrical Machines with Palermo University, Palermo, Italy, where he is also the Director of the Electrical Engineering Undergraduate Course. He has been consultant of many international governments. His main research interests include electrical drives, linear machines, magnetic materials, energy harvesting, electrical energy production from sea waves, medical equipment, and medical use of nuclear radiation.

Dr. Trapanese is a member of the Italian Standardization Body (CEI- Comitato Elettrotecnico Italiano) on photovoltaic and wind energy.

Valeria Boscaino was born in Palermo, Italy, in 1980. She received the master's degree in electronics engineering (summa cum laude) and the Ph.D. degree in electrical engineering from the University of Palermo, Palermo, in 2005 and 2009, respectively.

She is currently a Research Collaborator with the Department of Energy, Information Engineering and Mathematical Models, University of Palermo. Her research interests include modeling, analysis, design and control of power converters, fuel cell power systems, renewable energy sources, and electrical machines and drives.

Giovanni Cipriani was born in Palermo, Italy. He received the M.S. and Ph.D. degrees in electrical engineering from the University of Palermo, Palermo, in 2000 and 2014, respectively.

From 2002 to 2010, he was a High School Teacher in Electrotechnics. He has currently collaborated with the Department of Energy, Information Engineering and Mathematic Models, University of Palermo, on some research projects in collaboration with industries and research institutes. His research interests include converters, electrical machines and drives, PV plants, and linear motors.

Domenico Curto was born in Palermo, Italy, in 1990. He received the bachelor's (laude) and master's (laude) degrees from the University of Palermo, Palermo, in 2013 and 2015, respectively. He is currently working toward the Ph.D. degree with the University of Palermo.

His research interests include several multidisciplinary aspects as the designing and optimization of linear electrical machines, the exploitation of renewable energy sources with particular attention on sea wave and the analysis of energy savings in final users.

Vincenzo Di Dio received the M.S. and Ph.D. degrees in electrical engineering from the University of Palermo, Palermo, Italy, in 1993 and 1998, respectively.

From November 2000 to October 2004, he was a Postdoctoral Researcher with the Department of Electrical Engineering, Engineering College of Palermo. Since May 2006, he has been working with the University of Palermo as an Assistant Professor Converters, Electrical Machines, and Drives. He is currently an Assistant Professor of Electrical Machine and of Production of Electrical Energy from Renewable Sources. He is the scientific Supervisor of a research project in the field of smart cities. His main research interests include mathematical models of electrical machines, drive system control, and diagnostics, renewable energies, and energy management and linear machines particularly for generation of electricity from the waves.

Vincenzo Franzitta (M'13) received the M.S. and Ph.D. degrees in electrical engineering from the University of Palermo, Italy, in 1998 and 2001, respectively.

He is currently Associate Professor in University of Palermo, teacher of Technical Physics and Acoustic in Faculty of Engineering in the University of Palermo. His main research interests include energetic saving, environmental control and quality of life, and electrical energy production from sea wave energy; as well as energetics and management of the territory. He is a member of many research groups for national and international scientific cooperation among University of Palermo and others. He is the scientific manager of the Acoustical Laboratory and the La.Si.Tec.Ma. LAB (Marine Systems and Technologies Laboratory) of University of Palermo.